

PORTFOLIO

Music

Tiansheng Sun

www.tianshengs.com

LIST OF CONTENTS

Camera Calibration/Computer Vision Summer Research p4-5

Open Source GIS p6-8

Cartography Design p9-10

Hazards Research p11-14

P2-3
p3-5

Geologic Evolution of Vermont p15-16

Environmental Change of Lating America p17

Art History p18

Bioinformatics Algorithm p19

Music p20-24

PROJECT

Summer Research

Open Source GIS

Cartography Design

Hazards Research

Tiansheng Sun

Geologic Evolution

Environmental Change

Art History

Algorithm

www.tianshengs.com

Camera Calibration/Computer Vision Summer Research

Skill: computer vision, c++, openCV, camera calibration

<http://www.tianshengs.com/project/8.html>

In 2019, I undertook summer research on stereo vision with Professor Daniel Scharstein for the Middlebury Stereo Vision benchmark project. Specifically, I was in charge of designing and optimizing the camera calibration step, which estimates the intrinsic and extrinsic parameters of the camera system using calibration boards, most commonly a chessboard, which is highly accurate, or an Aruco board, which is less reliable but allows for occlusion of the board. One particular challenge I faced was when I placed the board too far from the camera, and the board could not be properly detected. To solve the problem, I created, printed, and experimented with self-designed Aruco chessboards where I placed Aruco codes in the setting of a chessboard, and ChaRuco boards, which combines the property of both a chessboard and an Aruco board, to increase detectability and accuracy. I also experimented with different settings and discovered that room setting, lighting, tilt of the board, the number of boards, the placement of boards, and the size of Aruco code all played a role in the detection of board markers. Finally, I wrote and refactored a program that prints the number of detected markers. The program prints out the number of detected markers while the user takes a set of images, output the number of detected markers, and warn the user to retake the image if the number of detected markers is too low. This specific step can improve the quality of data used for camera calibration, bringing more accurate result to the final analysis.

Github

- Camera Calibration

https://github.com/tianshengs/Camera_Calibration_MobileLighting2019

- SteamVR Tracking

https://github.com/tianshengs/SteamVR_Tracking

Camera Calibration/Computer Vision Summer Research

Skill: computer vision, c++, openCV, camera calibration

<http://www.tianshengs.com/project/8.html>



Generating High Quality Mobile Image Datasets for the Evaluation of Computer Vision Algorithms

Middlebury College Department of Computer Science
Summer 2019

Support through NSF Grant IIS-1718376 is gratefully acknowledged



Abstract

NYU research project aims to provide a system for capturing datasets to be used in the evaluation and testing of computer vision and related algorithms. The collected datasets will be composed of high-resolution ambient images captured by smartphones, fast and accurate depth maps generated by a structured lighting system. They will be evaluated as the core generalization of the well-known Middlebury Stereo Vision benchmarks, and are intended to address stereo and optical flow vision research by supplying highly accurate ground truth depth maps of static indoor scenes.

The main MobileLighting control program is written in Swift and C++ for macOS. It coordinates the different devices used for scene capture, including external projectors used to project structured lighting into the scene, a robot arm to move the smartphone, and an iDex (also known as iDex) which captures photos and IMU data.

To enable repeatable photo and video capture from highly constrained viewpoints and trajectories, the smartphone is mounted on the head of a UR5 robot arm. The arm aims to reproduce actual human arm trajectories recorded with SteamVR using an HTC VIVE tracker. After capture, the realistic kinetic data is smoothed and numerous reference points are chosen along the focal point's path. These trajectories are then loaded onto a Rosetta control server, which mediates communication between the two control programs and the robot.

Once the structured light images and ambient data have been collected in coordination with the projector, robot, and smartphone, the final program generates the image data to produce precise depth maps of the scene. In order to make the ground truth data as accurate as possible, the program produces camera calibration matrices to correct warping from the capture device's lens and differences in the relative angle of each viewpoint. These matrices are generated by comparing the calibration images taken by the system, a custom version of ArUco markers, pattern printed in downsampled images on flat boards.

Motivation

Research in multiview stereo vision and optical flow vision is held back by the absence of precise methods for evaluating the accuracy of different algorithms.

This project will fill that void by providing diverse datasets with subpixel accurate ground truth depth maps which researchers will be able to compare the results of their algorithms against.

The input (ambient) images provided will be true to modern mobile use cases, with images captured by mobile phones under a variety of different lighting conditions.

Calibration

The first step of the process involves taking images with specific coded patterns for intrinsic and extrinsic calibration, which calculates the intrinsic and extrinsic parameters of the camera model we are using.



Fig. 1a: Calibration process



Calibration Boards

For calibration purposes, we use our customized encoded ArUco boards. ArUco marker is a wide square marker with black corner and an inner binary matrix, which determines its unique ID, whose correspondence can be used for calibration purposes. It works successfully with partially occluded views. We have also experienced with ChArUco and Chessboard patterns.

Ground Truth

Ground Truth Calibration Problem

One of the major components required of the finished datasets is highly accurate ground truth depth information. There are a number of highly accurate systems available for 3D scanning. However, calibrating the output of any of these systems for comparison with the output of algorithms run on images from a camera can be daunting, especially when accounting for the relative location of depth sensors versus cameras.



Fig. 2: example of extrinsic calibration between camera and depth scanner that we avoid

Structured Lighting

To avoid the ground truth calibration problem, this system uses the same sensor (the smartphone camera) to obtain both ground truth depth information and stereo vision input images. In order to acquire ground truth, the program uses a "structured lighting" system which projects binary patterns onto the scene to get a unique pixel code for each point. The pixel codes are then compared between views; the more a pixel moves, the closer the surface is to the camera.



Fig. 3: projecting structured lighting onto a scene



Fig. 4: comparing 2D codes of points on image to extract depth information

Control and Coordination

The program is controlled from the central command-line application, MobileLighting Mac. MobileLighting Mac is responsible for commanding the smartphone for image capture, projecting structured lighting from the projectors (attached via a switcher box), commanding the UR5 robot via the Rosetta server, running calibration, processing the images, and recording all relevant scene data. MobileLighting Mac connects to MobileLighting iPhone and MLRobotControl wirelessly using network sockets.

Image capture occurs on a device running an iOS app, MobileLighting iPhone, which takes photos under various exposures and does some image processing automatically.

The movement of robot arm is controlled by the socket server, MLRobotControl, which is responsible for moving robot to specified viewpoint, executing pre-defined trajectories and sending the status of robot back to MobileLighting Mac.

MobileLighting Mac

- Command line tool
- Coordinates between different parts of the system, does image processing and calibration, records data.
- Written in Swift, C++, and Objective-C using Xcode.

MobileLighting iPhone

- iOS application
- Responsible for image capture and some image processing.
- Written in Swift using Xcode.

MLRobotControl

- Socket server
- Coordinates between the communication of robot and MobileLighting Mac, sends commands to robot arm
- Written in Python using Rosetta.

Viewpoint Management with UR5 Robot Arm

In order to have repeatable photo capture from different viewpoints, the smartphone is mounted on the tool head of a UR5 robot arm. Our main method of communicating with the robot arm is through Rosetta, a third-party robot programming environment based on ROS (Robot Operating System).

The robot arm can be instructed to move to a certain position in two different ways: joint positions and poses.

Joint Positions:

Since the robot arm has six joints, a position can be specified using an array of six angles, each represents the angle of a joint. This array gives a unique configuration of the robot arm. As a result, one option to define the viewpoints for the robot arm is to manually record a fixed number of joint positions and have the robot arm to move through them smoothly.

Poses:

The pose, on the other hand, contains an array with seven numbers. The first three numbers are the cartesian coordinate of the robot's tool head. The next four are the quaternions representing the orientations and rotations of the tool head in three dimensions. Therefore, another advanced option is to extract the human motion poses data using SteamVR with HTC VIVE tracker, then have the robot arm to mimic human motion as accurate as possible by passing the recorded data to Rosetta. The viewpoints will then be selected from the recorded trajectory.




Fig. 5: Smartphone mounting to the tool head




Fig. 6: Robot arm moving to different viewpoints during scene capture

VIVE Realistic Human Motion Tracking

To imitate the human arm motion and then execute the trajectory on the robot arm, VIVE tracker is used along with a base station to extract realistic pose information, which will then be passed to the UR5 robot arm through Rosetta. An image containing the information of the recorded trajectory will also be generated after saving the data. In Rosetta, the viewpoints will be selected according to the tracked poses.

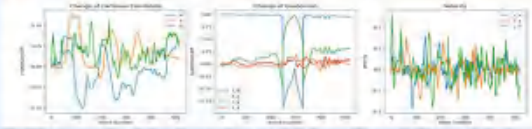


Fig. 7: The image generated that contains graphs showing the information of the recorded change of Cartesian Coordinates, change of quaternion, and velocity through time.




Fig. 8: the base station




Fig. 9: the motion tracker and sensor

Image Processing

To get ground truth depth maps of the highest possible quality, we use an image processing pipeline consisting of 6 steps:

Decode images

Decode the structured lighting images to get a unique pixel code for each point in the scene. This consists in projecting ever narrower lines in both the x- and y- directions (see fig. 3).

Rectify images

Using the extrinsic calibration parameters generated from calibration, rectify images from adjacent camera views so that they appear to lie on the same plane.

Disparity match images

Merge the x- and y- decoded images to get a unique pixel code for each point. Then compare the pixel codes from two views to get a disparity map.

Merge disparity maps

Merge disparity maps produced by different projectors to fill in as many depth values as possible as accurately as possible.

Reproject merged disparity maps

The merged disparities are used to self-calibrate the projector positions. Once the projector relationships are known, half-occluded regions can be filled in with disparity values.

Merge2

Put together original disparities, merged disparities, and reprojected disparities to fill in all possible values.

These steps are all implemented using C++ in MobileLighting Mac.

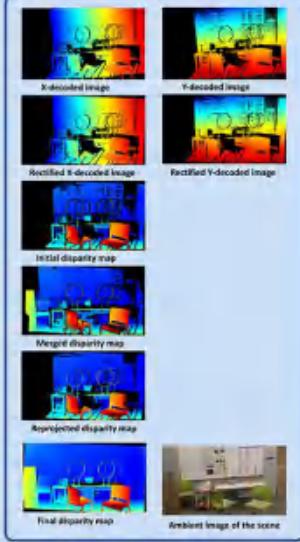


Fig. 10: the image processing pipeline

References

Fig 1b from <http://apps.man.poznan.pl/trac/stereovision>
Fig 2 from <https://iopscience.iop.org/article/10.1088/0957-0233/25/6/065107>
Fig 4 from https://link.springer.com/chapter/10.1007/978-1-4471-5520-1_6

Thanks to: Eamon McMahon for his help in mounting new ChArUco boards and Rick James for our WiFi routers.

Open Source GIS

Skill and Tools: GIS, SQL analysis, Batch Script, RStudio, QGIS

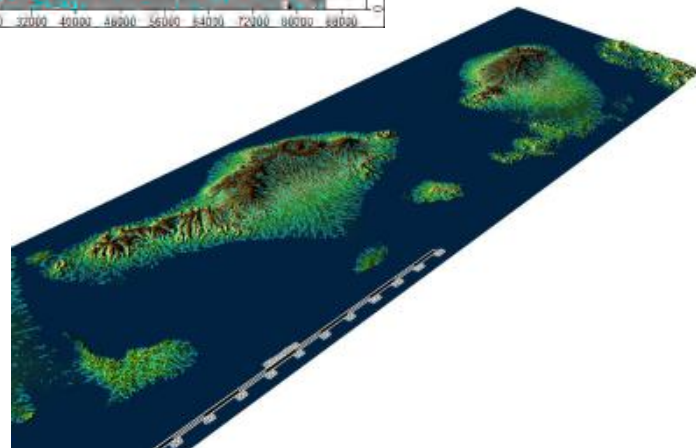
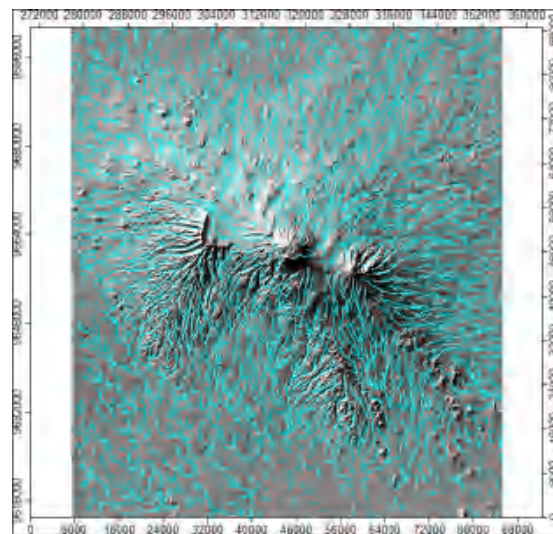
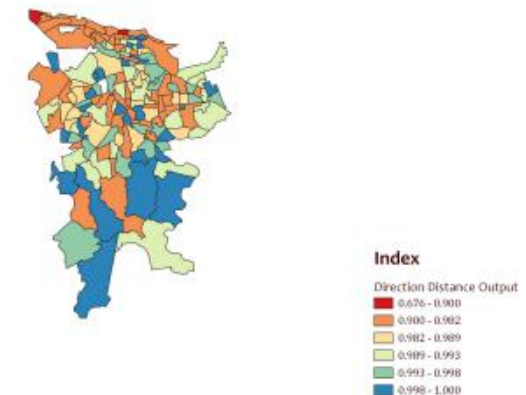
<https://tianshengs.github.io>

Activity 1: QGIS Modeling

<https://tianshengs.github.io/qgisModel.html>

I created a model to calculate the direction and distance from a point in QGIS. With the model, I downloaded data from Puerto Rico and did an analysis using the model that I made. Click to learn more.

Percentage of Hispanic Population in San Juan Metropolitan Area



Activity 2: Hydrology using SAGA

- Phase 1: Global Digital Elevation Models of Mt. Kilimanjaro

<https://tianshengs.github.io/globalDigitalElevation.html>

I used SAGA software to derive the channel networks of the Mt. Kilimanjaro region using SRTM data.

- Phase 2: Global Digital Elevation Models (Automation, Error Propagation and Uncertainty) of Bali and Lombok

<https://tianshengs.github.io/ModelErrorPropagation.html>

I used batch processing algorithms for SAGA tools to automate the processing tasks to calculate the channel networks of Bali and Lombok Islands, Indonesia, with a focus in understanding sources of errors and comparing elevation models and their resulting hydrological models from two different data sources (Aster and SRTM).

Open Source GIS

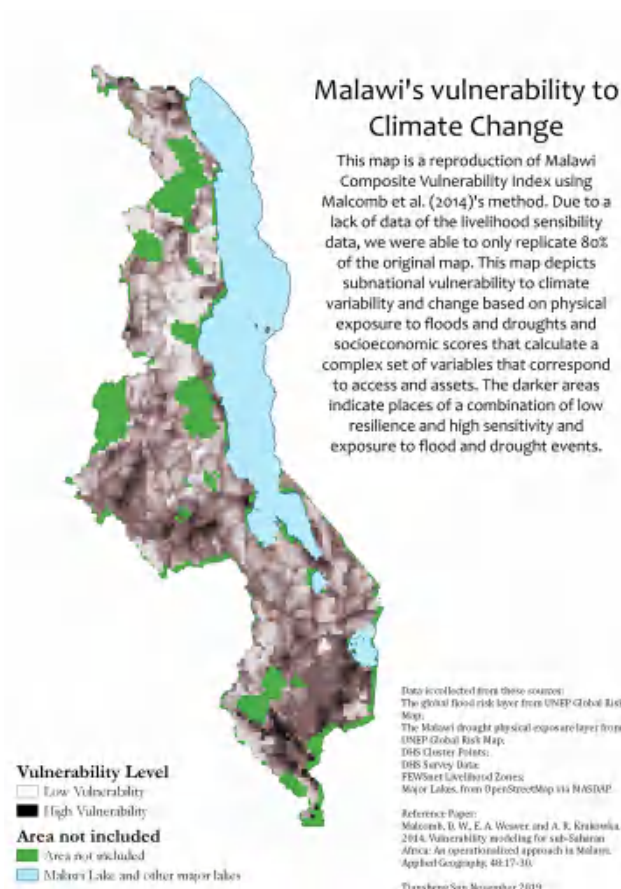
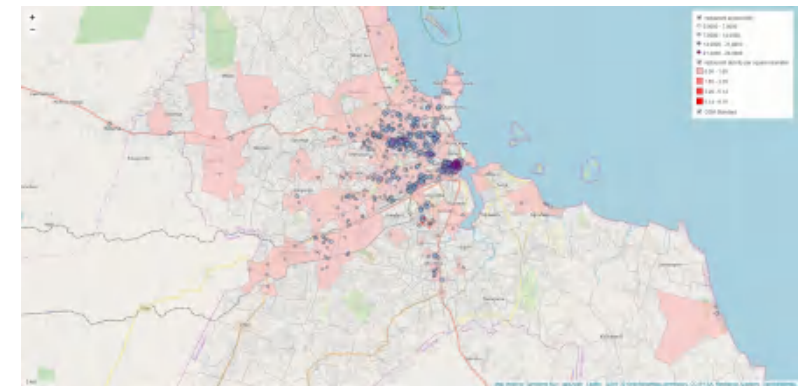
Skill and Tools: GIS, SQL analysis, Batch Script, RStudio, QGIS

<https://tianshengs.github.io>

Activity 3: Distribution of Hotels and Their Accessibility to Restaurants in Dar es Salaam

<https://tianshengs.github.io/DarAnalysis.html>

- Utilized PostGRESQL in QGIS to spatially analyze the spatial distribution of its hotels and their accessibility to the number of restaurants within 500-meter buffer using OpenStreetMap data.
- Created a Leaflet Map to visualize the final result of my analysis.



Activity 4: Vulnerability of Malawi

https://tianshengs.github.io/malawi_analysis.html

For this activity, I try to replicate the analysis of Malawi vulnerability of Malcomb et al.(2014)'s paper and critically understand the reproducibility and uncertainty of his approach.

Open Source GIS

Skill and Tools: GIS, SQL analysis, Batch Script, RStudio, QGIS

<https://tianshengs.github.io>

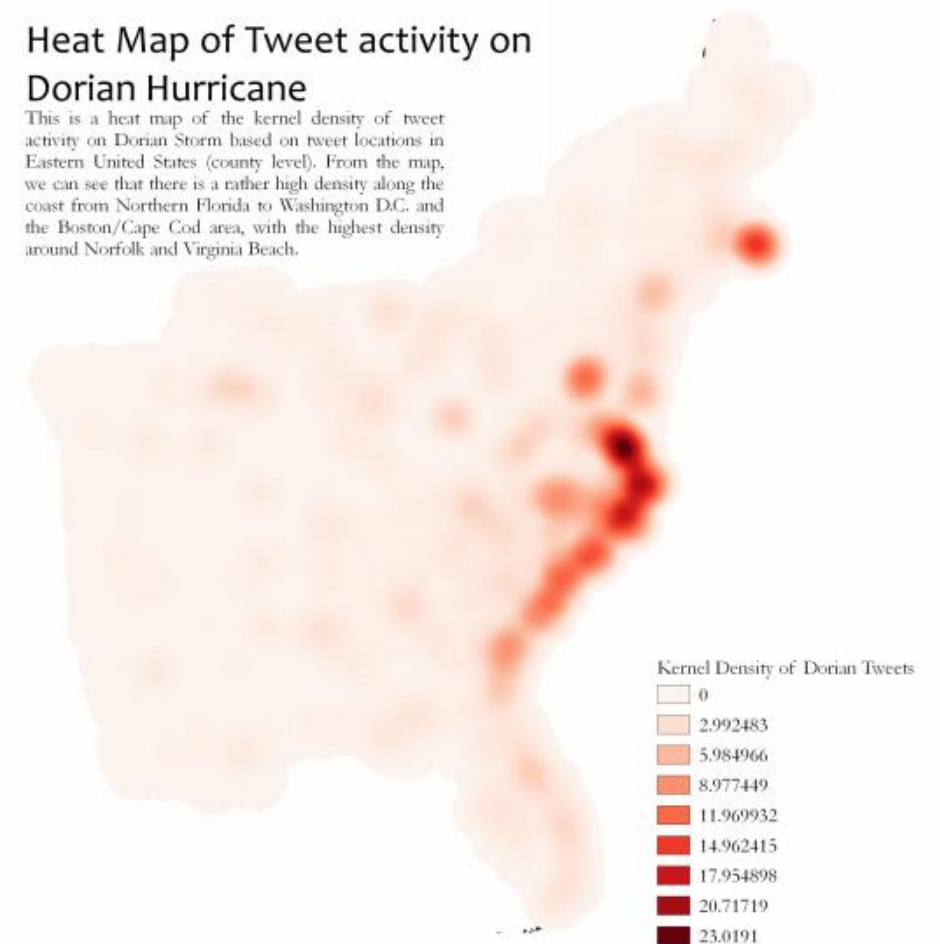
Activity 5: Sharpie versus Storm Surge in the Twittersphere of Hurricane Dorian

https://tianshengs.github.io/twitter_analysis.html

I conducted an analysis of the twitter activity during Hurricane Dorian to identify and map potential geographic clustering and hotspots of Twitter activity and think about whether the real hurricane path or President Trump's fake sharpie maps had driven more Twitter activity.

Heat Map of Tweet activity on Dorian Hurricane

This is a heat map of the kernel density of tweet activity on Dorian Storm based on tweet locations in Eastern United States (county level). From the map, we can see that there is a rather high density along the coast from Northern Florida to Washington D.C. and the Boston/Cape Cod area, with the highest density around Norfolk and Virginia Beach.



Activity 6: Christianity in Indonesia: A D3.js visualization

https://tianshengs.github.io/d3_indonesia.html

I learned how to make an interactive visualization using D3.js library and made a map showing the percentage of Christian people in each Indonesian province.

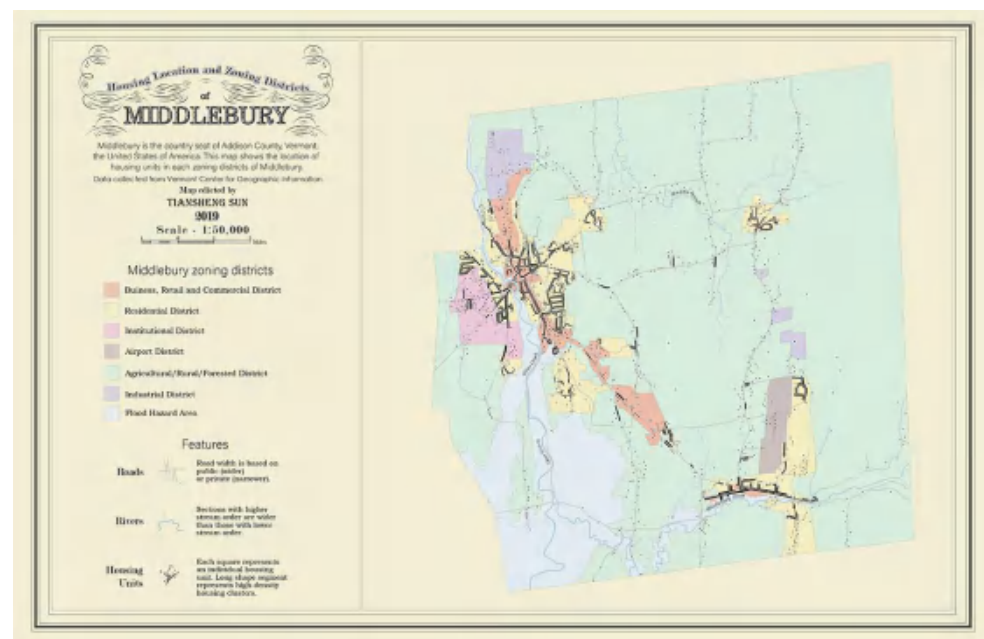
Cartography Design

Skill and Tools: GIS, SQL analysis, Batch Script, RStudio, QGIS

<http://www.tianshengs.com/project/11.html>

Niger River, the mother river of West Africa

This is a map showing Niger River and the cultural and physical geographic locations related to it.



Housing Location and Zoning Districts of Middlebury

This map shows the location of housing units in each zoning districts of the town of Middlebury, the country seat of Addison County, Vermont, USA.

Cartography Design

Skill and Tools: GIS, SQL analysis, Batch Script, RStudio, QGIS

<http://www.tianshengs.com/project/11.html>

The Timeless Continent

This article is a reproduction of a National Geographic map: the Timeless Continent. This maps show how time is used at Antarctic winter stations in 2009.



The Timeless Continent

Of the unusual phenomena that occur at the polar extremes of the Earth, time is a particularly peculiar one. Yes, the sky at the South Pole splits the year between whole days of light and dark. But how do humans who venture there—to a place where the world's 24 time zones converge—and to the rest of Antarctica set their clocks?

It all depends. While scientific observations follow coordinated universal time (UTC), each Antarctic research station (above, adopts one

of three practices for coordinating logistics on the ice. The majority keep the time of their home country. Others stay on the clock of the city from which their ships or aircraft departed. Fewer still use the standard time at their geographic location. All of which means a smattering of times on a continent the size of the United States and Mexico combined.

So who plays Father Time at the Pole itself? New Zealand, last port of call for Americans headed to their station at the bottom of the world. — Luna Shyr

MAP: Tiansheng Sun, Middlebury College
SOURCE: National Geographic



Map of Mauritania, Mali, Senegal, Gambia, Burkina Faso, and Guinea-Bissau

This is a reference map of the Sahel and Saharan region of West Africa, showing each countries' major cities, roads, airports, rivers and so on.

Vulnerability of Wuhan City to Waterlogging Event

Skill and Tools: LandSat image and classification tool in ArcMap.

<http://www.tianshengs.com/project/12.html>

This is my final paper for Human Geography of Hazards class in which I look into the vulnerability of Wuhan city to Waterlogging event. For the paper, I included the final research project I did for my Remote Sensing for Geoscience class as part of the evidence, in which I looked into the potential lake area change of Wuhan city as a whole and five specific lakes using LandSat image and classification tool in ArcMap.



Images of the Wuhan floods



The subway station in a commercial district in Wuchang was waterlogged

Vulnerability of Wuhan City to Waterlogging Event

Skill and Tools: LandSat image and classification tool in ArcMap.

<http://www.tianshengs.com/project/12.html>



The entire city is in great danger.

Abstract

In 2016, a series of unexpected storms paralyzed much of the City of Wuhan in central China, leading to severe waterlogging in the city (Figure 2.1, 2.2, and 2.3). The waterlogging event is believed to be the largest after the catastrophic 1998 flood when the entire city was heavily devastated. Though Wuhan is not the only victim of the 2016 waterlogging event, people raised their attention again to this large city in Central China, which has long been vulnerable to waterlogging caused by various flooding and storm events, including the 1931, 1954, and 1998 Yangtze river flood. This paper aims to understand Wuhan's waterlogging event, especially how inadequate research and the understanding of vulnerability, urban development and governmental policy and inadequacy lead to Wuhan's high vulnerability may increase its vulnerability.

Key words: Wuhan, vulnerability, flood, waterlogging, Urban development, Chinese politics

Vulnerability of Wuhan City to Waterlogging Event

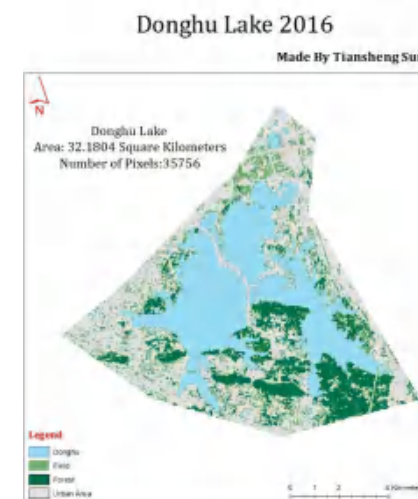
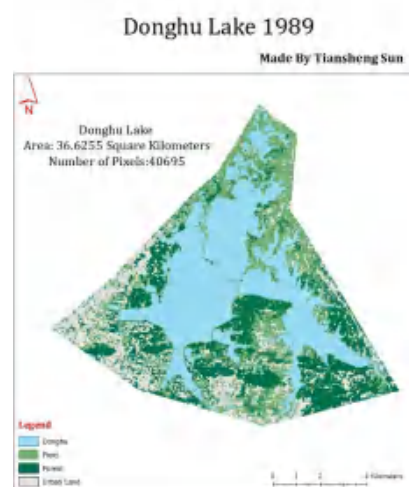
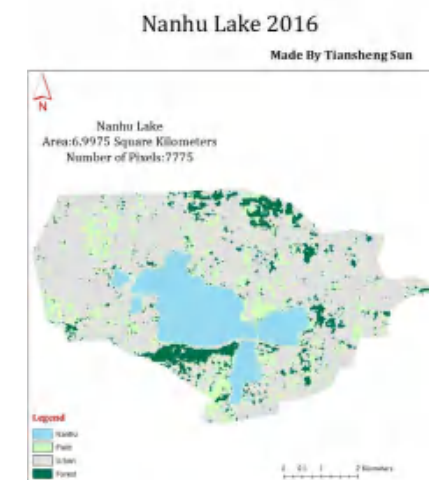
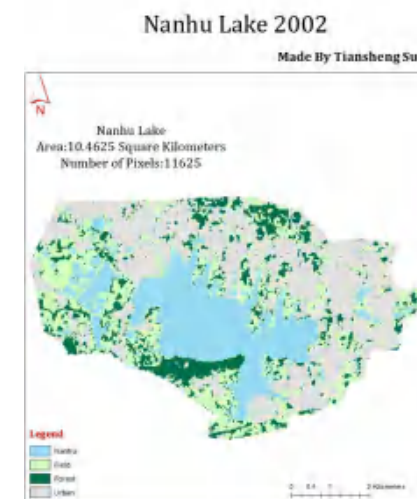
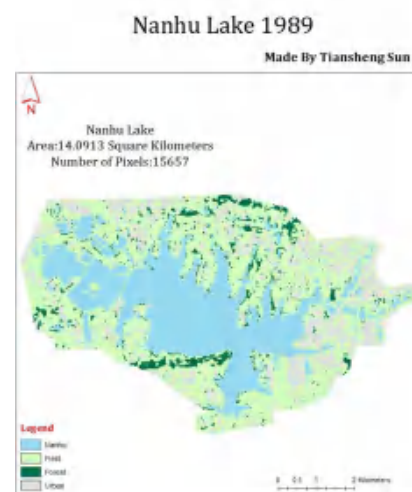
Skill and Tools: LandSat image and classification tool in ArcMap.

<http://www.tianshengs.com/project/12.html>

Wuhan's Shrinking Lake – Remote Sensing on Wuhan's 2016 Urban Waterlogging Event

I spearheaded the creation of classified maps of Wuhan City and four lakes: Nanhu, Shaihu, Shahu, and Donghu Lake using Landsat images in ArcMap. Moreover I handled the calculation and comparison of the total lake area and the four specific lakes in metropolitan Wuhan City, China in 1989, 2002 and 2016.

Nanhu images in 1989, 2002, and 2016



Donghu Images in 1989, 1998, and 2016

Vulnerability of Wuhan City to Waterlogging Event

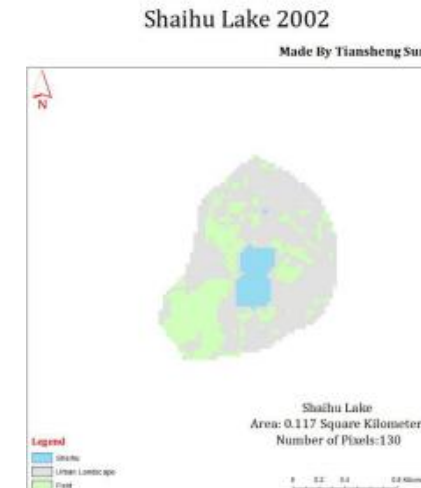
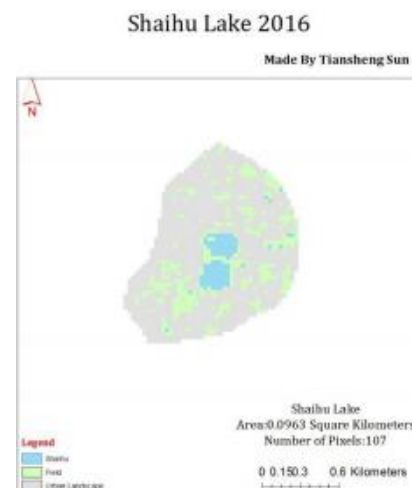
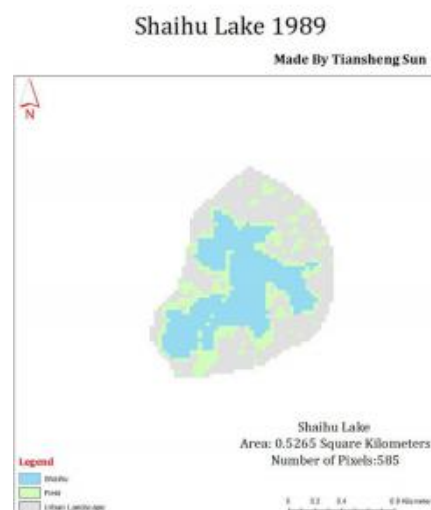
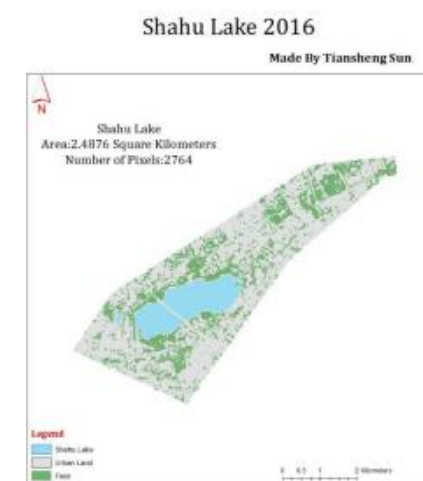
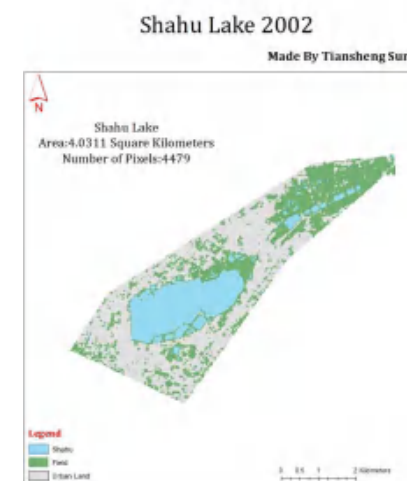
Skill and Tools: LandSat image and classification tool in ArcMap.

<http://www.tianshengs.com/project/12.html>

Wuhan's Shrinking Lake – Remote Sensing on Wuhan's 2016 Urban Waterlogging Event

I Spearheaded the creation of classified maps of Wuhan City and four lakes: Nanhu, Shaihu, Shahu, and Donghu Lake using Landsat images in ArcMap, moreover I Handled the calculation and comparison of the total lake area and the four specific lakes in metropolitan Wuhan City, China in 1989, 2002 and 2016.

Shahu Images in 1989, 1998, 2016



Shaihu Lake in 1989, 2002, 2016

Geological Evolution of Vermont

Skill and Tools: LandSat image and classification tool in ArcMap.

<http://www.tianshengs.com/project/14.html>



Abstract

This paper presents the geologic evolution of Vermont, U.S.A, from 565 Ma- 390 Ma for "Geology of Vermont". Sedimentary, metamorphic and igneous rocks formed at different period and environments were visited in six field trips around Vermont between September 21st, 2017 and Nov. 2nd, 2017. Descriptions of rocks presented in six geologic belts of Vermont give evidence to their environments of formation, which explain the tectonic evolution in the tectonic summary" section. The paper also pay attention to how geochemistry provides evidence of tectonic environment, and the role of Taconian Orogeny (470-460 Ma) and Acadian Orogeny (410-370) in reshaping the Vermont bedrock history. The appendices include complete field reports for the six field trips.

Keywords: Vermont, bedrock geology, Taconian Orogeny, Acadian Orogeny, tectonic environment

Geological Evolution of Vermont

Skill and Tools: LandSat image and classification tool in ArcMap.

<http://www.tianshengs.com/project/14.html>

<u>TITLE PAGE.....</u>	
<u>TABLE OF CONTENTS.....</u>	<u>1</u>
<u>1.ABSTRACT.....</u>	<u>1</u>
<u>2.INTRODUCTION.....</u>	<u>2</u>
<u>3.DATA.....</u>	<u>3</u>
3.1: PROTEROZOIC BASEMENT	3
3.2: CHAMPLAIN VALLEY BELT	3
3.2.1. CHESHIRE QUARTZITE AT THE ROCKY DALE	4
3.2.2. <i>MONKTON QUARTZITE AT THE REDSTONE QUARRY, THE SNAKE MOUNTAIN AND THE FRENCH FARM</i>	<i>4</i>
3.2.3. FORMATIONS EXPOSED AT CROWN POINT	5
3.3: TACONIC BELT	6
3.3.1. BULL FORMATION AND BROWNS POND FORMATION	6
3.3.2. WEST CASTLETON FORMATION AND HATCH HILL FORMATION	7
3.4: GREEN MOUNTAIN BELT.....	7
3.4.1. PINNACLE FORMATION	8
3.4.2. PINNEY HOLLOW FORMATION	8
3.5: ROWE HAWLEY BELT	8
3.5.1. STOWE FORMATION	9
3.5.3. MORETOWN FORMATION	9
3.6: CONNECTICUT VALLEY BELT	10
3.6.1. PLYMOUTH GRANITE	10
3.7: BRONSON HILL BELT.....	10
3.8: TACONIAN OROGENY AND ACADIAN OROGENY	11
<u>4.TACTONIC SUMMARY.....</u>	<u>12</u>
<u>REFERENCE CITED.....</u>	<u>14</u>
<u>FIGURES</u>	

<u>FIG. 1 GEOLOGIC MAP OF VERMONT.....</u>	
<u>FIG. 2 STRATIGRAPHIC COLUMNS OF VERMONT</u>	
<u>FIG. 3 TECTONIC INFORMATION AT 565 MA</u>	
<u>FIG. 4 TECTONIC INFORMATION AT 530 MA</u>	
<u>FIG. 5 TECTONIC INFORMATION AT 490 MA.....</u>	
<u>FIG. 6 TECTONIC INFORMATION AT 465 MA</u>	
<u>FIG. 7 TECTONIC INFORMATION AT 450 MA</u>	
<u>FIG. 8 TECTONIC INFORMATION AT 420 MA.....</u>	
<u>FIG. 9 TECTONIC INFORMATION AT 400 MA.....</u>	
<u>FIG. 10 TECTONIC INFORMATION AT 390 MA</u>	

<u>APPENDICES</u>	
APPENDIX 1: LIMESTONE IN CROWN POINT	
APPENDIX 2: MONKTON QUARTZITE	
APPENDIX 3: TACONIC SEQUENCE IN THE FAIR HAVEN AREA.....	
APPENDIX 4: METAMORPHIC ROCKS IN CENTRAL VERMONT	
APPENDIX 5: ROCKS NEAR LINCOLN GAP ALONG NEW HAVEN RIVER	
APPENDIX 6: UNDERSTAND THE PLYMOUTH GRANITE	

Chan Chan and El Niño: A historical perspective and modern lessons

<http://www.tianshengs.com/project/13.html>



This is my final paper for my Environmental Change of Latin America class, in which I looked into the case of Chan Chan and how its story provides policy maker a unique perspective for environmental awareness in our modern world.

Executive Summary

El Niño events are not a modern phenomenon, but a long established one. Residents of Chan Chan of the Chimú civilization in pre-Columbian Peruvian coast were among the ones who faced threats from these events. Its story, therefore, is important to our understanding of these events which become increasingly strong in recent years and can provide a lesson of how we may deal with them in contemporary time. With increasing value in tourism, Chan Chan, now as an archaeological zone, should also be used as a site of environmental awareness, educating both the local residents and tourists.

Vermeer and Procelains

<http://www.tianshengs.com/project/12.html>

The paper in which I looked into how Chinese procelains and Delftware had influenced Vermeer's paintings.



*Johannes Vermeer,
Woman with a Pearl
Necklace, 1662-
1665,
Gemäldegalerie,
Berlin*



*Johannes Vermeer,
Young Woman Reading
a letter at an Open
Window, 1657-1658,
Gemäldegalerie Alte
Meister, Dresden*



*Johannes Vermeer,
The girl with a Wine
Glass, 1661-1662,
Herzog Anton Ulrich
Museum,
Braunschweig*



*Johannes Vermeer,
The Procuress,
1656, Gemäldegalerie
Alte Meister, Dresden*


Neighbor-Joining Algorithm and its application in bioinformatics algorithm'

This is for the final paper the for which I looked at the neighbor joining algorithm and ran the algorithm on data collected from the MEGA software for the Ebola event in 2012 and the SARs outbreak in 2003 to a construct a revolutionary tree for both events.

Neighbor Joining Algorithm and its applications in Phylogenetic tree construction

Tiansheng Sun
Department of Computer Science, Middlebury College

Introduction



Where did human come from?

When did HIV jump from primates to humans?

HIV

A phylogenetic tree can answer these questions. Phylogenetic trees tell us evolutionary relationships among different entities by looking at their genetic similarities and differences.

SPECIES	ALIGNMENT	DISTANCE MATRIX
Chimp	ACGTAGGCCT	Chimp 0 3 6 4
Human	ATGTAAGACT	Human 3 0 7 5
Seal	TCGAGAGCAC	Seal 6 7 0 2
Whale	TCGAAGCAT	Whale 4 5 2 0

Seems like we can construct a distance matrix where the distance between two species is the number of differing symbols between them. We can then use the distance matrix to make a phylogenetic tree by looking at the smallest value using some algorithms similar to hierarchical clustering?

DISTANCE MATRIX
A B C D
A 0 3 6 4
B 3 0 7 5
C 6 7 0 2
D 4 5 2 0

This example suggests that although it looks intuitive that the smallest element in the distance matrix correspond to a pair of neighbors in a revolutionary tree, this is not always the case. Therefore, we need another method to deal with this problem.

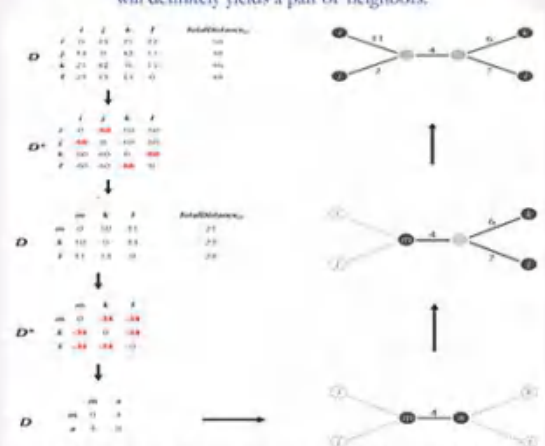
The data for this project is collected from NCBI, access from MEGA. A MEGA 4 is also used to align genes for this project. Graph is drawn manually.

Acknowledgement:
Thank you Professor Lindebaum for the support of this project.

Reference:
Compeau, P and Pevzner, P (2010). Bioinformatics Algorithms: An Active Learning Approach, 111-117. Active Learning Publishers.
Nei, M, and Nei, M (1997). The neighbor-joining method: a new method for reconstructing phylogenetic trees. Molecular Biology and Evolution, 14(6), 406-425.
Polygenetic Tree Practical Problem. Access from https://bioinformaticspractical.com/active_learning/Evolution%20Practical%20Polygenetic%20Tree%20Practical%20Problem.pdf

Neighbor Joining Algorithm

Neighbor Joining Algorithm was developed by Naruya Saitou and Masatoshi Nei in 1987 for revolutionary tree construction. It has been cited for over 50,000 times, and is one of the most quoted paper cited in all of science (Compeau and Pevzner, 2018). Since finding a minimum element in a distance matrix D does not guarantee a pair of neighbors, Neighbor Joining Algorithm transforms distance matrix D into a different matrix D* whose minimum element will definitely yields a pair of neighbors.



Source: Compeau, P and Pevzner, P (2010). Bioinformatics Algorithms: An Active Learning Approach, 176. Active Learning Publishers

Steps:

- From $n \times n$ matrix D constructs $n \times n$ matrix D^* , such that:

$$D^*_{ij} = (n-2) * D_{ij} - \text{TOTALDISTANCE}(i) - \text{TOTALDISTANCE}(j)$$
- Find the minimum value of D^* at row a and column b and transform the initial $n \times n$ matrix into a new $(n-1) \times (n-1)$ matrix by replacing a and b with a new leaf c.
- Calculate the limb length of the new leaf c to the deleted leaves a and b, as paired neighbors, using these functions:

$$\Delta_{ab} = (\text{TOTALDISTANCE}(i) - \text{TOTALDISTANCE}(j)) / (n-2)$$

$$\text{LimbLength}(a,c) = 0.5 * (D_{ab} + \Delta_{ab})$$

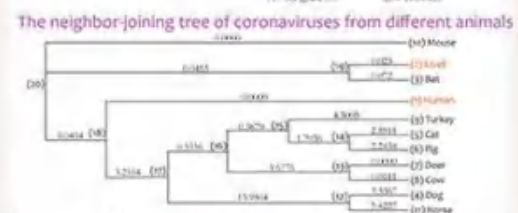
$$\text{LimbLength}(b,c) = 0.5 * (D_{ab} - \Delta_{ab})$$
- Repeat the first three steps until we get a 2×2 distance matrix D which corresponds to a tree with a single edge.
- Add all pairs of neighbors to our polygenetic tree.

Biological applications

Which animal gave us SARs?

Data	Animal	Output
Accession Number	Animal	
AY274119	Human	14-151.7576
AY304486	Cover	15-151.7576
KY417144	Bar	15-151.7576
GQ477367	Dog	15-151.7576
MG605090	Cat	15-151.7576
KC242792	Pig	15-151.7576
FJ425190	Deer	15-151.7576
DR811784	Cow	15-151.7576
EU022526	Turkey	15-151.7576
DQ497008	Mouse	15-151.7576
LC061273	Horse	15-151.7576

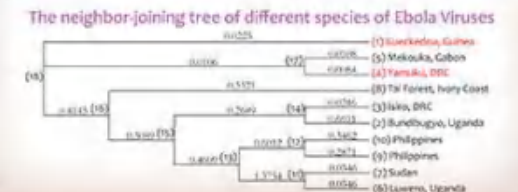
The neighbor-joining tree of coronaviruses from different animals



Which species of Ebola viruses caused the 2012 Ebola outbreak?

Data	Virus Species	Date	Output
Accession Number	Virus Species	Date	
KJ660348	EBV	2014	15-151.7576
FJ217161	BDBV	2007	15-151.7576
KC545393	BDBV	2012	15-151.7576
AF273001	EBOV	1976	15-151.7576
KC242792	EBOV	1994	15-151.7576
KC589025	SUDV	2012	15-151.7576
FJ968794	SUDV	1976	15-151.7576
FJ217162	TAFV	1994	15-151.7576
AF522874	RESTV	1990	15-151.7576
FJ621583	RESTV	2008	15-151.7576

The neighbor-joining tree of different species of Ebola Viruses



MUSIC

Piano Performances

Carillon Performances

Tiansheng Sun

Piano Concert

Certification

www.tianshengs.com

Piano Performances

- Enrique Granados: 4. Quejas, o La Maja y el ruiseñor from Goyescas, Op. 11

<https://youtu.be/YhuAz1eVBPc>

- J.S.Bach, French Suite in G Major BWV816: Sarabande & Gavotte

<https://youtu.be/uwUwuXT9xr4>

- Gabriel Fauré, Nocturne in E-Flat, Op.36

<https://youtu.be/aW3kB1UJF4U>

- Debussy-La plus que lente (Valse)

<https://youtu.be/gKNGYCciOw>

- Beethoven Moonlight- Sonata Op. 27 No. 2

https://youtu.be/MD_DKaNCy6s

- Chopin's nocturnes- Op.62 No.2

<https://youtu.be/OqSHfB2lhcs>

- Scarlatti-Sonata In A Major, K.208, L.238

<https://youtu.be/gwXKazehx0Y>

- PARTITA1

<https://youtu.be/wUtHQ0ryWBA>

- PARTITA2

https://youtu.be/Uqf3bb_4KwU





Carillon Performances

- Liling Huang, Belfry Sketches

<https://youtu.be/IOvwcN-h5Ls>

Piano Concert

Music is flowing painting and painting is the art of solidification of music.

This concert is using piano hearing art to express the spectacular movement of visual art.

- Complete video of the concert

<https://www.youtube.com/watch?v=vdm3X8OdDD4&feature=youtu.be>

- Short video of the concert

<https://www.youtube.com/watch?v=vtL8a5EfGMg&feature=youtu.be>





Certification

Licentiate of the Royal Schools of Music for Music Performance: Piano

Tiansheng Sun

Tiansheng Sun

www.tianshengs.com